

$$\begin{aligned}
W_4 &= 16F_{13} + 2F_{17} + 2F_{37} + 6F_{12} - 2F_{15}, & B_2 &= 2F_{56} + 2F_{15} - F_{25}, \\
W_5 &= 2F_{35} + 8F_{28} + 8F_{18} - 5F_{17} - 5F_{26} + 8F_{16} - 2F_{15} & B_3 &= 4F_{56} - F_{57}, \\
&\quad + 4F_{25} + 4F_{12} + 2F_{34}, & B_4 &= 4F_{15} - 8F_{13} + 2F_{17} - F_{37}, \\
W_6 &= 6F_{13} + 12F_{12} - F_{57} - 3F_{26} + 2F_{15} + 4F_{27} + 4F_{25}, & B_5 &= F_{17} + F_{26} - F_{35} - 4F_{23} - 4F_{13} + 2F_{16} - 2F_{15} + 4F_{25} \\
&\quad + 12F_{25} + 2F_{26} + 4F_{56} + 4F_{67}, & &\quad + 2F_{34} + 4F_{12}, \\
W_7 &= 8F_{27} + 4F_{16} + 12F_{23} - 2F_{17} - 6F_{15} - 2F_{57} + 12F_{12} & B_6 &= 4F_{25} + 4F_{27} - 4F_{15} - F_{57}, \\
&\quad + 12F_{25} + 2F_{26} + 4F_{56} + 4F_{67}, & B_7 &= 2F_{27} + 4F_{16} - 2F_{17} - 2F_{57} - 4F_{26} + 4F_{56} + 4F_{69}, \\
W_8 &= 16F_{35} + 8F_{13} + 8F_{23} + 4F_{37} + 8F_{56} + 4F_{12} + 2F_{57} & B_8 &= 2F_{57} + 4F_{15} + 4F_{25} - 2F_{17} + 4F_{27} - 8F_{35} - 4F_{13} \\
&\quad - 2F_{15} - 2F_{25} - 2F_{17} + 4F_{27}, & &\quad - 4F_{23} - 2F_{37} + 8F_{56} + 4F_{12}, \\
B_0 &= 2F_{56} + F_{57}, & \text{where} & \\
B_1 &= 8F_{12} + 2F_{17} + F_{67} - F_{27} - 4F_{26}, & F_{ij} &= -V_0 \exp(-\kappa r_{ij}^2).
\end{aligned}$$

PHYSICAL REVIEW

VOLUME 124, NUMBER 2

OCTOBER 15, 1961

Once-Forbidden Beta Spectrum of Tl²⁰⁶†

D. A. HOWE AND L. M. LANGER

Physics Department, Indiana University, Bloomington, Indiana

(Received June 9, 1961)

The beta spectrum of 4.2-min Tl²⁰⁶ was investigated in a 4 π scintillation spectrometer. The source was in secular equilibrium with the 2.6 $\times 10^6$ year Bi²¹⁰ parent. The electron distribution was observed to have a nonstatistical form which could be fitted with a once forbidden pseudovector shape factor. No necessity for the inclusion of any pseudoscalar contribution was observed. The energy release in the Tl²⁰⁶ decay is 1.571 \pm 0.010 Mev.

INTRODUCTION

A DETAILED study of the Tl²⁰⁶ beta spectrum has been made in a 4 π scintillation spectrometer. A nonstatistical distribution was observed which could be fitted with a pseudovector shape factor. The energy release in the decay of Tl²⁰⁶ was found to be 1.571 \pm 0.010 Mev.

The beta decay of Tl²⁰⁶ to Pb²⁰⁶ is described as a 0⁻ \rightarrow 0⁺ transition. According to the $V-A$ law,¹⁻⁵ only the pseudovector (A) coupling can appreciably influence the decay. If a pseudoscalar coupling were also to exist, this would also contribute, and many authors have used the 0⁻ \rightarrow 0⁺ transition as tests of this point.⁶⁻¹⁰ It will be shown that the nonstatistical

shape of the Tl²⁰⁶ beta spectrum can be explained in terms of a pure pseudovector shape factor with no pseudoscalar contribution. Indeed, it would be an error to include the pseudoscalar interaction without also considering higher order terms in the pseudovector contribution.

Originally, this study was undertaken in order to determine the energy released in the Tl²⁰⁶ decay with greater accuracy. The knowledge of the end point is important in locating the energy levels of Bi²¹⁰. One state of Bi²¹⁰, the 5-day RaE isomer, decays by β emission to Po²¹⁰. Po²¹⁰ alpha decays to Pb²⁰⁶. The total energy release in this branch is 6.460 \pm 0.006 Mev. The 2.6 $\times 10^6$ -yr isomer of Bi²¹⁰ decays by α emission to Tl²⁰⁶. Tl²⁰⁶ decays to Pb²⁰⁶. At the time when work was started on this problem, it was believed that the (4.930 \pm 0.010)-Mev α group of Bi²¹⁰ (2.6 $\times 10^6$ yr half-life) decayed to the ground state of Tl²⁰⁶. The end point of the Tl²⁰⁶ β spectrum had been reported as 1.51 \pm 0.01 Mev.¹¹ The end point of the Tl²⁰⁶ β spectrum had been reported as 1.51 \pm 0.01 Mev.¹¹ Thus the total energy released in this branch was 6.440 \pm 0.020 Mev. Since the energy released in the two branches was the same within the experimental errors, it was not clear which of the two isomers is the ground state of Bi²¹⁰. An accurate determination of the end-point energy of the β spectrum of Tl²⁰⁶ would possibly remove this uncer-

† Supported by the joint program of the Office of Naval Research and the U. S. Atomic Energy Commission.

¹ M. E. Rose, *Handbook of Physics* (McGraw-Hill Book Company, Inc., New York, 1959), pp. 9-90.

² E. J. Konopinski, *Ann. Rev. Nuclear Sci.*, **9**, 99 (1959).

³ M. Deutsch and O. Kofoed-Hansen, *Experimental Nuclear Physics*, edited by E. Segrè (John Wiley & Sons, Inc., New York, 1959) Vol. III, pp. 427-638.

⁴ Y. Smorodinskii, *Uspekhi Fiz. Nauk* **67**, 1 (1959).

⁵ D. L. Pursey, *Proc. Roy. Soc. (London)* **A246**, 444 (1958).

⁶ C. P. Bhalla and M. E. Rose, *Phys. Rev.* **120**, 1415 (1960).

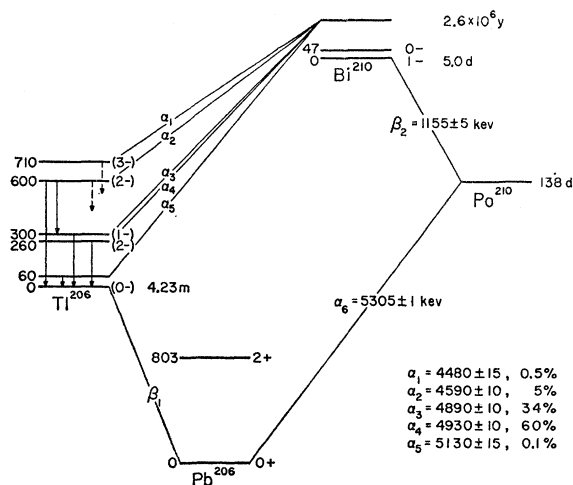
⁷ J. H. Hamilton and L. M. Langer, *Bull. Am. Phys. Soc.* **3**, 208 (1958).

⁸ R. L. Graham, J. S. Geiger, and T. A. Eastwood, *Can. J. Phys.* **36**, 108 (1958).

⁹ F. T. Porter and P. P. Day, *Phys. Rev.* **114**, 1286 (1959).

¹⁰ L. N. Zyiriconova, *Izvest. Akad. Nauk S.S.S.R., Ser. Fiz.* **20**, 1399 (1956) [translation: *Bull. Acad. Sci., Phys. Ser. U.S.S.R.* **20**, 1280 (1956)].

¹¹ D. Alburger and G. Friedlander, *Phys. Rev.* **82**, 977 (1951).

FIG. 1. Decay scheme of Bi^{210} .

tainty. During the course of this investigation, it was shown by Golenetskii *et al.*^{12,13} that the α spectrum of Bi^{210} is complex and that all the α transitions go to excited states of Tl^{206} (Fig. 1). In particular, the most intense α group (4.930 ± 0.010 Mev) is in coincidence with 260-kev gamma rays. Thus the energy released in the Bi^{210} (2.6×10^6 yr half-life) $\rightarrow \text{Tl}^{206} \rightarrow \text{Pb}^{206}$ branch is larger by 260 kev than was previously thought. The energy released in the 2.6×10^6 -yr Bi^{210} branch is 6.761 ± 0.017 Mev and that of the 5-day RaE branch is 6.460 ± 0.006 Mev. Therefore, 5-day RaE is the ground state of Bi^{210} and the 2.6×10^6 -yr half-life isomer of Bi^{210} is an excited state located 301 ± 20 kev above the ground level of Bi^{210} .

Earlier investigations¹¹ report that Tl^{206} decays with a half-life of 4.23 min. The same authors report no gamma rays and that the beta spectrum has a statistical shape above 600 kev. Even so, it will be shown that the data of Alburger and Friedlander are better fitted by the shape factor reported in this paper. Because the half-life is so short, it is difficult to measure the shape of the beta spectrum by conventional methods.

The method employed by Alburger and Friedlander is to produce Tl^{206} in a reactor from Tl^{205} and transfer the source to a magnetic spectrometer. This procedure has several disadvantages. Since the half-life is so short, no chemical separation can be performed. Thus the source is thick and may contain impurities. Also, the activity decays so rapidly that there is not enough time to measure the complete spectrum with a single source; several bombardments must be made in order to cover the entire energy range. Some method must be used to normalize all of these runs to the same source strength.

¹² S. V. Golenetskii, L. I. Rusinov, and Yu. I. Filimonov, J. Exptl. Theoret. Phys. (U.S.S.R.) **37**, 560 (1959) [translation: Soviet Phys.-JETP **10**, 395 (1960)].

¹³ S. V. Golenetskii, L. I. Rusinov, and Yu. I. Filimonov, J. Exptl. Theoret. Phys. (U.S.S.R.) **35**, 1313 (1958) [translation: Soviet Phys. JETP **8**, 917 (1959)].

The method used in this experiment is to analyze the beta spectrum from Tl^{206} in secular equilibrium with the 2.6×10^6 -yr half-life isomer of Bi^{210} . In any conventional magnetic spectrometer, a source of long-lived Bi^{210} of sufficient intensity would be too thick for definitive spectrum shape measurements. If instead a scintillation spectrometer with 100% transmission is used, a source strength of about 10 μC would be sufficient. This amount of Bi^{210} can be spread as a thin source over an extended area. One difficulty with this method is that the α particles from Bi^{210} and Compton electrons from the associated gamma rays will be detected by the scintillation spectrometer. It will be shown that these do not influence the spectrum above 600 kev.

APPARATUS

In the present experiment, all spectrum measurements were made with a 4π beta-ray scintillation spectrometer similar to that described by Johnson *et al.*¹⁴ The major differences are that 5-in. photomultiplier tubes and 3.5-in. diameter $\times \frac{1}{2}$ -in. plastic scintillators are used. Early tests with DuMont 6364 photomultiplier tubes and NE102 plastic scintillators showed a resolution of 40% for the Cs^{137} internal-conversion line in this experimental arrangement. Tests with a small NaI(Tl) crystal indicated that the main source of line broadening was the nonuniformity of response of the 6364 photocathode. The use of a logarithmic spiral light pipe gave more uniform illumination of the photocathode regardless of the origin of the light pulse in the scintillator and improved the resolution considerably. It was then found that EMI 9579B photomultiplier tubes have very uniform photocathodes. The use of these tubes greatly improved the resolution and eliminated the necessity for the cumbersome light pipes. Indeed, the resolution of the system was found to be better without the light pipes, which introduce some loss of intensity because of imperfect transmission in the optical system. The final resolution was 18%.

Figure 2 shows a block diagram of the 4π beta-ray scintillation spectrometer used in this experiment. Both photomultipliers received light from each event observed

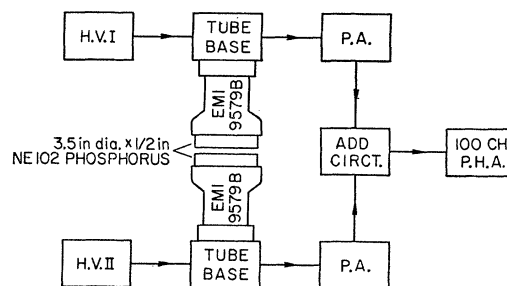


Fig. 2. A block diagram of the scintillation spectrometer. The source is located between the two scintillators.

¹⁴ R. G. Johnson, O. E. Johnson, and L. M. Langer, Phys. Rev. **97**, 1031 (1955).

by the scintillators. The pulses from the two photomultiplier tubes are combined in a linear addition circuit.¹⁴ The summed pulse goes through a linear amplifier and is then analyzed by a 100-channel pulse-height analyzer. The photomultiplier tubes were found to be more stable with positive high voltage. In addition, it was found that the resistor chain shown in Fig. 3 gave better resolution and stability than the voltage networks previously used at this laboratory.

The two high-voltage supplies were adjusted for minimum width of the 624-kev internal conversion line and were monitored with a potentiometer throughout all experimental runs.

The scintillation counters were completely enclosed by a lead shield 2 in. thick. This was lined on the inside with a $\frac{1}{8}$ -in. layer of steel.

EXPERIMENTAL MEASUREMENTS

A sample containing about 50 mg of bismuth which gave a total of 8.0×10^8 alpha disintegrations per min was obtained from I. Perlman. The sample had been made by $\text{Bi}^{209}(n, \gamma)\text{Bi}^{210}$ for other studies on Bi^{210m} and rigorously purified.¹⁵ This gives 8.0×10^8 beta particles per min distributed over the entire spectrum of Tl^{206} . The source material was spread over a large area ($\sim 20 \text{ cm}^2$) in order to reduce the source thickness as much as possible. The Bi^{210m} source was made into a series of concentric rings of 2.5-in. maximum diameter on a backing of $\frac{1}{4}$ -mil Mylar, covered with a thin ($\sim 20 \mu\text{g}/\text{cm}^2$) layer of Zapon. An insulin solution was used to define the source and aid in spreading it uniformly. The source was then covered with a layer of $\frac{1}{4}$ -mil Mylar for symmetry and to protect the source from damage and the plastic scintillators from contamination.

Because this method of source distribution was new, it was necessary to check the calibration and linearity of the spectrometer. Sources of Cs^{137} and Bi^{207} were prepared in an identical manner to that used for the Tl^{206} source. The 624-key internal conversion line of

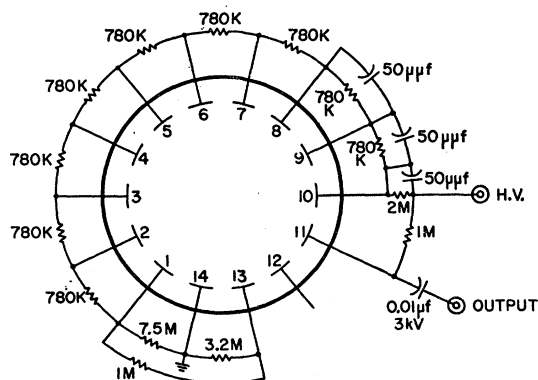


FIG. 3. The voltage divider used with the EMI 9579(B) photomultiplier tubes.

¹⁵ H. B. Levy and I. Perlman, Phys. Rev. **94**, 152 (1954).

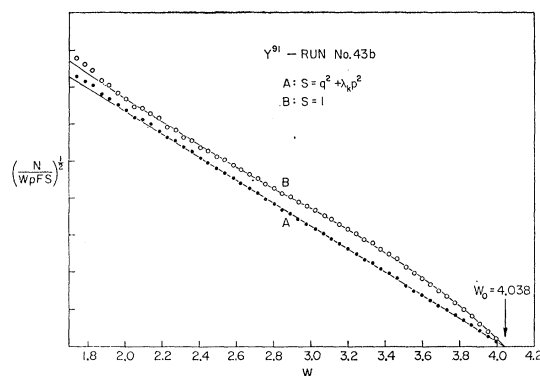


FIG. 4. Fermi-Kurie plot of a typical Y^{91} run. Curve A shows the linearization provided by the application of the unique once forbidden shape factor.

Cs^{137} and the 976-keV internal conversion line of Bi^{207} were used as calibration points. A similar source of Y^{91} was prepared. The beta spectrum of Y^{91} has a once-forbidden unique shape. Figure 4 shows the Fermi-Kurie plot obtained for the Y^{91} spectrum. It is clear from the curve having the $S=q^2+\lambda_k p^2$ shape factor applied that a once-forbidden unique spectrum is observed. Here, q is the neutrino momentum, p is the electron momentum, and λ_k is a slowly varying function of the electron energy W , which has been tabulated by Kotani.¹⁶ In addition, the Y^{91} end point is very close to the Tl^{206} end point and can be used as an additional calibration point. As a check on the stability of the spectrometer, the Y^{91} spectrum was measured before and after each measurement of the Tl^{206} spectrum.

Figure 5 shows the Fermi-Kurie plot of Tl^{206} . The excess counts at low energies are the result of Compton electrons from the gamma rays and alpha particles which are also stopped in the scintillators. A calibration with Po^{210} alpha particles showed that pulses from the Bi^{210m} alpha particles will not distort the spectrum above 600 kev. The second curve of Fig. 5 shows the effect of adding $\frac{3}{4}$ -mil Mylar (sufficient to stop all the alpha particles) to each side of the source.

The background was reduced to approximately 10% of the beta counting rate by the shielding used. The background was subtracted automatically by the 100-channel analyzer.

EVIDENCE FOR A $0^- \rightarrow 0^+$ TRANSITION IN Ti^{206}

The decay scheme of $\text{Bi}^{201m} \xrightarrow{\alpha} \text{Tl}^{206} \xrightarrow{\beta} \text{Pb}^{206}$ is shown in Fig. 1. The spins and parities of the ground state and first-excited state of Pb^{206} are well established. The ground state of this even-even nucleus is 0^+ . The first-excited state has been established as 2^+ by α - γ angular correlation measurements¹⁷ made on Po^{210} . Measurement of the multipole order and the K/L ratio

¹⁶ T. Kotani and M. Ross, Phys. Rev. **113**, 622 (1959).

¹⁷ S. DeBeneditti and G. H. Minton, Phys. Rev. **85**, 944 (1952).

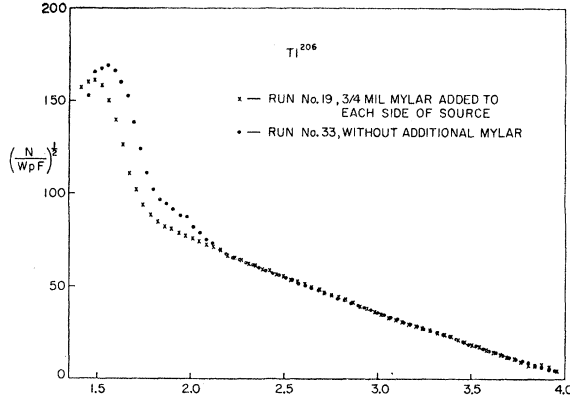


FIG. 5. Fermi-Kurie plot of the Tl^{206} spectrum. The plot is unchanged above 600 kev when $\frac{3}{4}$ mil of Mylar is added to each side of the source. This shows that the α particles from Bi^{210} that are detected by the scintillators do not distort the spectrum above this point, and that the effective thickness of the source is not influencing the spectrum above 600 kev.

of the 803-kev gamma transition confirm this assignment.¹⁸

The ground state of Tl^{206} must either be 0^- or 1^- . If the spin of the ground state of Tl^{206} were 1^- , then the beta transition to the 2^+ level of Pb^{206} should have an ft value close to that for the transition to the ground state of Pb^{206} . Each would be a $\Delta I=1$ (yes) transition. Using $W_0=4.075$ it is found that $\log ft=5.25$ for Tl^{206} . If the decay were also to go to the first excited state of Pb^{206} there would be 773 kev available. If the $\log ft$ were about 5.3 for this group, this transition should make up 11% of the decays. If this were the case, the 803-kev gamma ray should be observed. If the $\log ft$ for the transition were as large as 7, this transition would make up 0.2% of the decays, and the gamma ray should still be easily detectable.

A strong Tl^{206} source was prepared by $\text{Tl}^{205}(n,\gamma)\text{Tl}^{206}$ reaction and quickly transferred to a gamma counting chamber. A search with a NaI(Tl) detector and 100-channel pulse-height analyzer of the gamma spectrum revealed no gamma ray above the bremsstrahlung spectrum. A gamma ray with 0.2% intensity would have been easily detected. On the other hand, if the ground state of Tl^{206} is 0^- , a transition to the 2^+ level would be once-forbidden unique, $\Delta I=2$ (yes), and would account for only 0.001% of the total decays. This is consistent with the gamma-ray observations. Thus, it can be concluded that the ground state of Tl^{206} is probably 0^- .

On the basis of the nuclear-shell model, taking pairing interactions and the interaction with the nuclear surface into account, Kharitonov¹² has calculated a doublet structure of levels for Tl^{206} that leads to a $s_{\frac{1}{2}}$ proton hole and $p_{\frac{1}{2}}$ neutron-hole configuration for the ground state. Application of Nordheim's strong rule gives the spin and parity as 0^- for the ground state of Tl^{206} .

¹⁸ D. E. Alburger, *Beta and Gamma Ray Spectroscopy*, ed. by K. Siegbahn (Interscience Publishers, Inc., 1955), Ch. XXII.

Studies of α - γ coincidences¹² from Bi^{210m} are consistent with the assignment of 0^- to the ground state.

$0^- \rightarrow 0^+$ SHAPE FACTOR

Experiments¹⁻⁵ of the last few years lead to the $V-1.2A$ interaction in beta decay. At the present time the only conclusion that can be made about the contribution of the pseudoscalar interaction, if it exists at all, is that its effect on the shape of the beta-ray spectrum appears to be small.

Transitions of the type $0^- \rightarrow 0^+$ are once forbidden. The pseudovector coupling contributes appreciably only through the matrix elements $\langle \sigma \cdot r \rangle$ and $\langle \gamma_5 \rangle$. If the pseudoscalar interaction exists, it will contribute through $\langle \beta \gamma_5 \rangle$.

The pseudovector shape factor can be written

$$S_A = K_A [b_0 + b_1 \lambda^2 + b_2 \lambda], \quad (1)$$

where the following definitions are used:

$$K_A = C_A^2 \left(i \int \sigma \cdot r \right)^2,$$

$$\lambda = - \int \gamma_5 / i \int \sigma \cdot r, \quad (2)$$

$$b_0 = M_0 - \frac{2}{3} q N_0 + \frac{1}{9} q^2 L_0,$$

$$b_1 = L_0 + \frac{2}{3} q R (N_0 R) + \frac{1}{9} q^2 R^2 (M_0 R^2) + (2/9) p^2 R^2,$$

$$b_2 = -2 \{ N_0 [1 - (4/9) q^2 R^2] - \frac{1}{3} q (L_0 - M_0 R^2) \}.$$

The expressions M_0 , N_0 , and L_0 are the usual combinations¹⁹ of the radial wave functions, evaluated through order R^2 :

$$\begin{aligned} M_0 R^2 &\approx \frac{1}{2} (1 - \gamma) + \alpha Z R / (2\gamma + 1) [(2\gamma - 1) W - \gamma / W] \\ &\quad + \frac{1}{9} p^2 R^2 + \dots, \\ N_0 R &\approx -\frac{1}{2} \alpha Z - R / (2\gamma + 1) [(2\gamma^2 + \gamma - 2) W - \gamma / W] \\ &\quad + (11/18) \gamma \alpha^2 p^2 R^2 + \dots, \\ L_0 &\approx \frac{1}{2} (1 + \gamma) - \alpha Z R / 2(\gamma + 1) [(2\gamma + 3) W + \gamma / W] \\ &\quad - \frac{1}{3} p^2 R^2 + \dots, \end{aligned} \quad (3)$$

where R is the nuclear radius measured in units of \hbar/mc . The expressions b_0 , b_1 , and b_2 contain terms that are usually omitted from the pseudovector shape factor²⁰ as it generally appears in the literature.⁶ The usual approximation is valid only for $|\lambda| \ll 1$.

Substitution of the electron radial functions (3) into the shape factor (1) yields, correct through order R ,

$$\begin{aligned} S_A &= (K_A / R^2) \{ \frac{1}{2} (1 - \gamma) + \frac{1}{3} \alpha Z R (p^2 / W) + \frac{1}{3} q R \alpha Z \\ &\quad + (\lambda R)^2 [\frac{1}{2} (1 + \gamma) - \frac{1}{3} \alpha Z R (5W + 1/W) - \frac{1}{3} q R \alpha Z] \\ &\quad + (\lambda R) [\alpha Z + \frac{2}{3} R (p^2 / W) + \frac{2}{3} q R] \}. \end{aligned} \quad (4)$$

¹⁹ E. J. Konopinski and G. E. Uhlenbeck, Phys. Rev. **60**, 308 (1941).

²⁰ E. J. Konopinski (private communication).

Equation (4) can be expressed in the form

$$S_A = (K_A/R^2)T\{1+aW+b/W\}, \quad (5)$$

where the following definitions have been used:

$$\begin{aligned} a &= -\frac{4}{3}\alpha ZR(\lambda R)^2/T, \\ b &= \frac{1}{4}a[1+2/\lambda R\alpha Z+1/(\lambda R)^2], \\ T &= (\frac{1}{2}\alpha Z+\lambda R)^2+\frac{2}{3}W_0R(\lambda R). \end{aligned} \quad (6)$$

In Eq. (6) the approximation

$$\gamma \approx 1 - \frac{1}{2}\alpha^2 Z^2 \quad (7)$$

has been used. The first term of T in Eq. (6), $(\frac{1}{2}\alpha Z+\lambda R)^2$, must be larger than $\frac{2}{3}W_0R(\lambda R)$ for the neglect of still higher order terms (in R) to be valid. Also, one notices that a in Eq. (6) can only take on negative values; thus, only shape factors having negative slopes can be explained by Eq. (5). Because b/W is a small perturbation to aW it will only determine whether the shape factor plot turns up or down at low energies.

The terms that must be added to the shape factor (1) if the pseudoscalar interaction exists are

$$\Delta S = K_A[b_3\xi^2 + (b_4+b_5\lambda)\xi] + \dots, \quad (8)$$

where $\xi = C_P/MC_A$, M is the nucleon mass, and C_P and C_A the pseudoscalar and pseudovector coupling constants. The coefficients b_3 , b_4 , and b_5 are functions of radial wave functions similar to those for b_0 , b_1 , and b_2 .⁶ The second term in (8), $(b_4+b_5\lambda)$, arises from the interference between the pseudovector and pseudoscalar interactions.

ANALYSIS OF THE DATA

Because of the finite resolution of the spectrometer, it is necessary to make certain corrections to the observed data. All spectrum measurements were corrected for instrument resolution by the method of Palmer and Laslett.²¹ The correction is small for all

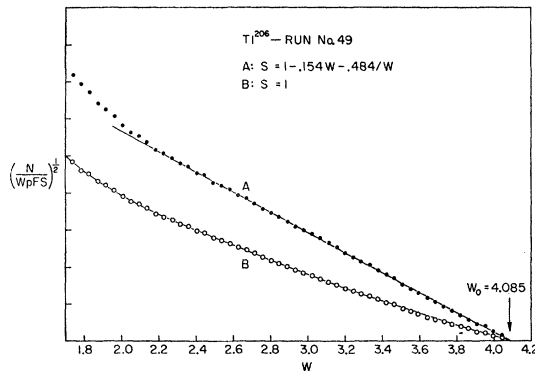


FIG. 6. Fermi-Kurie plots of the Ti^{206} beta spectrum. Curve A shows that the pseudovector shape factor, $S=1-0.154W-0.484/W$, yields a linear Fermi-Kurie plot above 600 kev. Curve B is a conventional Fermi-Kurie plot ($S=1$).

²¹ J. P. Palmer and L. J. Laslett, U. S. Atomic Energy Commission Bulletin ISC-174, 1950 (unpublished).

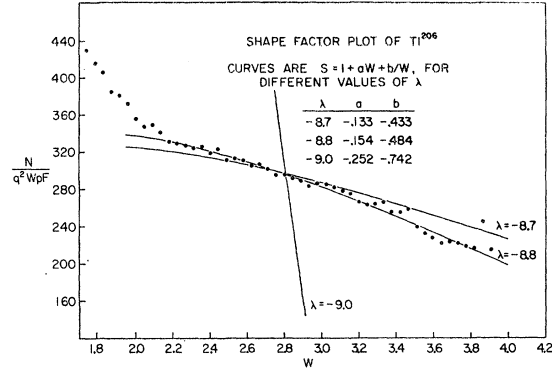


FIG. 7. Shape factor plot of Ti^{206} data. Curves for $\lambda = -8.7$, -8.8 , and -9.0 show the strong dependence of the shape factor on λ .

experimental data except the last few points near the end point of the spectrum. For the data exhibited here, the correction was less than 1% throughout the body of the spectrum. This correction and the Fermi-Kurie (F-K) plot were calculated with the aid of an IBM 650 computer. Fermi functions, $F(Z,W)$, were calculated for each datum point by the computer. Figure 6 shows the Fermi plot obtained for one of the experimental runs on Ti^{206} .

An experimental shape factor $S_E = N/q^2WpF$ is shown in Fig. 7. The value of the maximum energy W_0 has been adjusted as a slight parameter in order to maintain a smooth behavior in the energy region near the end point. The experimental shape can be fitted by a shape factor of the form

$$S = 1 + aw + b/W, \quad (9)$$

where a and b are related by Eq. (6). Values of a and b for a best fit are

$$a = -0.154, \quad b = -0.484. \quad (10)$$

The a and b given in Eq. (10) correspond to $\lambda = -8.8$. These values are consistent with an end point $W_0 = 4.075 m_0c^2$.

The second curve of Fig. 6 shows the F-K plot of Ti^{206} with this shape factor applied.

Alburger and Friedlander¹¹ reported a statistical shape for Ti^{206} . A close examination of their data reveals that their F-K plot is indeed curved, but because of possible source thickness and the sparsity of data points they reported no deviation from a statistical shape. Their F-K plot is reproduced in Fig. 8. The second curve shows the result of applying the shape factor found in the present investigation [Eq. (10)]. Thus, the data of Alburger and Friedlander are also consistent with the shape factor $1-0.154W-0.484/W$. When this shape factor is applied, their end point agrees with the maximum energy found in the present experiment to within 5 kev.

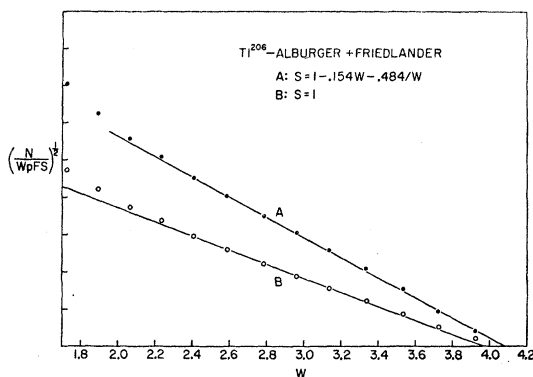


FIG. 8. Fermi-Kurie plot of Tl^{206} data reported by Alburger and Friedlander. Curve B shows the conventional plot of the data. Curve A shows a plot after the application of the shape factor found in this investigation. The data now extrapolate to a higher end point in good agreement with the value found in the present study.

CONCLUSION

The beta spectrum of Tl^{206} has been measured and was found to have a nonstatistical shape. The data are

fitted by a pure pseudovector shape factor

$$S = 1 - 0.154W - 0.484/W.$$

No pseudoscalar contribution is needed in order to fit the spectrum.

With the measured energy release 1.571 ± 0.010 Mev it is possible to make a better determination of the first-excited state of Bi^{210} . Using the energies reported by Golenetskii *et al.*¹² the long-lived metastable state of Bi^{210} is found to be 301 ± 10 kev above the ground level.

ACKNOWLEDGMENTS

The authors are indebted to Dr. I. Perlman of the Berkeley Radiation Laboratory for supplying the sample of long-lived isomer of Bi^{210} used in this experiment and to Professor M. B. Sampson and the cyclotron group for making the bombardments. The authors also wish to thank Professor E. J. Konopinski for many helpful discussions and for calculating the corrections to the pseudovector shape factor.

Nuclear Quadrupole Moment of Fe^{57m}

GERALD BURNS

International Business Machine Research Center, Yorktown Heights, New York

(Received June 9, 1961)

A value for the nuclear quadrupole moment of the excited state of iron, Q^{57m} , is obtained using published values for eQq/h in the octahedral and tetrahedral sites in $Y_3Fe_2(FeO_4)_3$ (YIG) and in Fe_2O_3 , along with recent values for the atomic coordinates in these compounds. The value of Q^{57m} is definitely positive and $\approx +0.4 \times 10^{-24}$ cm².

INTRODUCTION

THE Mössbauer effect¹ enables one to obtain values of the nuclear quadrupole coupling constant, eQq/h . This quantity is a measure of the interaction of the nuclear quadrupole moment, Q , with the second derivative of the electrostatic potential along a particular crystal direction, q . Kistner and Sunyar² were the first to measure eQq/h of the excited nuclear state of iron 57, Fe^{57m} . The excited state has a nuclear spin, I , of $\frac{3}{2}$ and can thus possess a nonzero Q .

In this paper an estimate of Q^{57m} is made using the following published data for eQq/h : measurements of Fe in both Fe_2O_3 by Buchanan and Wertheim,³ and in the octahedral and tetrahedral sites in $Y_3Fe_2(FeO_4)_3$ (YIG) by Alff and Wertheim.⁴ In all of these cases the iron is

in a +3 valence state. This simplifies the calculation since the outer electron configuration is a half-filled $3d$ configuration; thus the unperturbed core contribution to q is zero. The contribution to q then arises from the other ions in the lattice. One can then obtain q as follows:

$$q = (1 - \gamma_\infty) \sum_i \left(\frac{3 \cos^2 \theta_i - 1}{r_i^3} \right) e_i \equiv (1 - \gamma_\infty) q_u, \quad (1)$$

where γ_∞ is the antishielding factor,⁵ r_i is the distance to the i th charge, θ_i is the angle between the principal axis of the field gradient tensor and r_i , e_i is the charge of the i th ion and the sum is over all the ions in the lattice except the one at $r=0$. The antishielding factor for Fe^{+3} has already been calculated.⁶ The lattice sum is calculated on an IBM 704 using a program developed by Bersohn.⁷

¹ R. L. Mössbauer, *Z. Physik* **151**, 124 (1958).

² O. C. Kistner and A. W. Sunyar, *Phys. Rev. Letters* **4**, 412 (1960).

³ D. N. E. Buchanan and G. K. Wertheim, private communication (to be published).

⁴ C. Alff and G. K. Wertheim, *Phys. Rev.* **122**, 1414 (1961); also, G. K. Wertheim, private communication.

⁵ H. M. Foley, R. M. Sternheimer, and D. Tycko, *Phys. Rev.* **93**, 734 (1954); R. M. Sternheimer and H. M. Foley, *ibid.* **102**, 731 (1956); and R. M. Sternheimer, *ibid.* **84**, 244 (1951).

⁶ G. Burns and E. G. Wikner, *Phys. Rev.* **121**, 155 (1961).

⁷ R. Bersohn, *J. Chem. Phys.* **29**, 326 (1958).